Materials Research. 2017; 20(3): 613-618
DOI: http://dx.doi.org/10.1590/1980-5373-MR-2015-0732

Optical and Structural Properties of Natural $MnSeO_4$ Mineral Thin Film

Ishak Afşin Kariper*[a]

[a] *Erciyes University, Education Faculty, 38039, Kayseri, Turkey*

Received: December 01, 2015; Revised: January 26, 2017; Accepted: February 18, 2017

Manganese selenite ($MnSeO_4$) crystalline thin film has been produced with chemical bath deposition on substrates (commercial glass). Properties of the thin film, such as transmittance, absorption, and optical band gap and refraction index have been investigated via UV/VIS Spectrum. The structural properties of orthorhombic form have been observed in XRD. The structural and optical properties of $MnSeO_4$ thin films, deposited at different pH levels were analyzed. Some properties of the films have been changed with the change of pH level, which has been deeply investigated. The grain size of $MnSeO_4$ thin film has reached its highest value at pH 9. The refraction index and extinction coefficient of $MnSeO_4$ thin films were measured to be 1.53, 2.86, 2.07, 1.53 (refraction index) and 0.005, 0.029, 0.014, 0.005 (extinction coefficient) for grain sizes 21, 13, 26, and 5 nm respectively. The band gaps (Eg) of the films were measured to be 2.06, 2.57, 2.04, and 2.76 eV for the grain sizes mentioned above. The value of dielectric constant at pH 10 was calculated as 1.575.

Keywords: *Crystal growth, thin films, chemical synthesis, X-ray diffraction, optical spectroscopy*

1. Introduction

Selenium is one of the most important elements of 6A group in periodical table in terms of utilization areas. This element and his compounds, including selenite, have various characteristics. Selenate can be obtained from a salt or ester by replacing one or both hydrogen of selenic acid with metal ions or with an organic group. Selenate, unlike sulfate, is a good oxidizer and can be easily reduced to selenite or selenium. Selenium's valence can be reduced from +6 to +4 and -2 by removing the oxygen atoms, but it is really difficult to reduce its valance from +6 to -2. Some chemical properties of selenate are similar to sulfate. But, unlike sulfate, metallic compounds of selenate are not soluble in water. Cadmium, copper, nickel and manganese selenite are analogues of each other. These are known as metallic salts of selenic acid. Metals are bond to the oxygen atoms of selenite anion[1,2].

Researchers have worked on the thermo-gravimetric analysis of some divalent metals' selenite, obtained by the hydration and decomposition of manganese (II), cobalt, nickel, copper (II), and zinc cadmium and cobalt selenite[3]. Other researchers investigated metal selenite as open-framework materials which are showing interesting physical properties[4]. Moreover, some of them worked on the biologic effects of selenite on cells[5]. But, nobody examined optical properties of metal selenite (especially manganese selenite) up to now.

On the other hand, being easy to produce, low cost and not harmful for human health, natural mineral oxide thin films have become a focus of subject of the researchers. These kind of metal oxide materials may be very useful in technology because they are used as p-type absorber in solar batteries, detectors and sensors. P-type absorbing materials, which have a high production cost, are much-needed in the technology; thus the manufacturing of them, where there is a shortcoming, has a particular significance. The most common example of them is Cu_2O thin films[6-10]. This mineral, which is widely present in the nature, is a quite stable compound. Therefore, with the addition of required chemicals, copper can be easily transformed into its oxide in aqueous media. On the other hand, heating at high temperatures and adding much more chemicals are needed for the production of other metal oxide materials. Therefore, the production of natural mineral thin films poses a particular importance for technology[11-14].

In this study, structural and optical properties natural $MnSeO_4$ mineral thin films, which were produced via chemical bath deposition method, have been investigated. The pH value of the bath has been used to control structural and optical properties of $MnSeO_4$ thin films. Chemical bath deposition method has been preferred because it is a simple and cheap method, and as far as we know nobody has produced natural $MnSeO_4$ mineral thin films up to now neither with this method, nor using other ones.

2. Experimental

The preparation and production of selenite anions is the most important stage of this method. 0.01 mol solid selenium was dissolved in the water with 0.04 mole potassium hydroxide, which was four times more concentrated than selenium. But, since the pH level of the bath was very high for the deposition, 5 mL HCl solution was added in order

* e-mail: akariper@gmail.com

to decrease the pH value to 11. As another component of the bath, 0.01 M manganese nitrate solution was prepared. Then, 20 mL selenite solution and 20 mL manganese solution (with equal concentration) were mixed in a beaker. Glass substrates of 76x26 mm, soaped with detergent and rinsed with distilled water, were dipped into this bath.

The pH levels of the baths were set as 10, 9 and 8, by adding 2, 4 and 8 mL of 8% HCl solution. The temperature and deposition time was set as 4 hours and 50°C for all baths. The pH levels of the chemical baths were measured using a pH meter (Lenko mark 6230N).

The crystalline structure of the $MnSeO_4$ was confirmed by X-ray diffraction (XRD) with a $CuK\alpha_1$ radiation source (Rikagu RadB model, λ=1.5406 Å) over the range $10^o < 2\theta < 90^o$ at a speed of 3^o min^{-1} with a step size of 0.02^o. The optical measurements were determined by Hach Lange 500 Spectrophotometer at room temperature by placing an uncoated identical commercial glass substrate in the reference beam. The optical spectrum of thin films was recorded in the wavelength range of 300-1100 nm.

3. Results and Discussion

The chemical reactions occurred during the bath deposition are summarized below. When manganese ions (Mn^{+2}) is added to the solution containing selenate (SeO_4^{-2}) the precipitation of manganese selenite ($MnSeO_4$), which is not soluble in water, is observed.

$$Se_{(k)} \xrightarrow{KOH/H2O} SeO_4^{-2}{}_{(aq)} \quad (1)$$

$$Mn^{+2}{}_{(aq)} + SeO_4^{-2}{}_{(aq)} \longrightarrow MnSeO_{4(k)} \quad (2)$$

Equations (1) and (2) show the formation of SeO_4^{2-} and $MnSeO_4$. In an aqueous environment with a basic solution, selenium is dissolved in the form of selenite anions.

Figure 1 displays XRD patterns of various $MnSeO_4$ thin films, produced at different pH levels, using chemical bath deposition method (a: pH 11, b: pH 10, c: pH 9, d: pH 8). In addition, the comparisons of these peaks with ASTM values are given in Table 1. Nearly, amorphous structures were observed at pH 11, 9 and 8, but it was comparatively lower at pH 10 where the highest peak was observed. Thus, the method and the bath prepared at pH 10 can be set as a specific methodology for the production of $MnSeO_4$ thin films. An orthorhombic structure was observed with the indexing of the structure on XRD EVA program (a= 4.93, b= 9.13, c= 7.02 Å; Z: 4). The comparison of XRD results with ASTM values fitted well with standard values.

For all films, grain size (D), which is the structural parameter, were evaluated by XRD patterns and presented in Figure 2. The grain size of the thin films was calculated from XRD patterns using Debye Scherrer's formula[15],

$$D = \frac{0.9\lambda}{B\cos\theta} \quad (3)$$

where D is the grain size, λ is the X-ray wavelength used, β is the angular line width at half-maximum intensity in radians and θ is Bragg's angle. The grain size of the films is calculated using the peaks of FWHM (020) at pH 11, (021) at pH 10, (111) at pH 9 and (022) at pH 8, obtained through the Scherrer's method which takes peaks of XRD patterns.

The highest average grain size of $MnSeO_4$ thin films has been found at pH 9. The average grain sizes of the thin films are 21, 13, 26, and 5 nm for pH 11, 10, 9 and 8 respectively. The reason of the low grain sizes at pH 10 and 8 is the strength of crystallization peaks. The dominance of crystal structure to amorphous structure is another reason. When the average grain sizes get smaller, the grains stack more stringently, which causes the spaces between grains to decrease. Thus, the deposition of the film on such structures leads to more orderly structures. This can be seen on XRD patterns as well. So, the peaks that we have observed at pH 10 are in line with the obtained results.

The optic band gap energy (Eg) was calculated from the absorption spectra of the films using the following relation[16,17]:

$$(\alpha h\nu) = A(h\nu - Eg)^n \quad (4)$$

Where A is a constant, α is absorption coefficient, hν is the photon energy and n is a constant, equal to ½ for direct band gap semiconductor. The plot of $(\alpha h\nu)^2$ versus hν is drawn in figure 3 (a: pH 11, b: pH 10, c: pH 9, d: pH 8).

Plot of $(\alpha h\upsilon)^2$ vs. hυ for $MnSeO_4$ films at different pH levels (a) pH 11, (b) pH 10, (c) pH 9, (d) pH 8 is displayed in figure 3. As mentioned before, we were able to control the structures of the films by controlling pH levels of the baths. This caused variations on the grain sizes for each pH level and optic band gaps have been varied accordingly. Optic band gaps of the films are 2.76, 2.57, 2.06 and 2.04 eV for average grain sizes 5, 13, 21, 26 nm, respectively. As can be seen, the grain size is inversely correlated with optical band gap, which were also observed by other researchers before. The quantum size has affected optic band gap[18].

The transmittance (T) of $MnSeO_4$ thin film can be calculated using reflectivity (R) and absorbance (A) by the following expression[16,17]:

$$T = (1-R)^2 e^{-A} \quad (5)$$

Figures 4 and 5, show the transmittance, reflectance and the absorbance of $MnSeO_4$ thin films obtained from baths with different pH levels. The lowest transmittance and the highest reflectivity values were observed at pH 10. This is due to the fact that the absorption of light by crystal structure is higher. The absorption curve behaved as the reflectance curve and showed an increase with the decrease

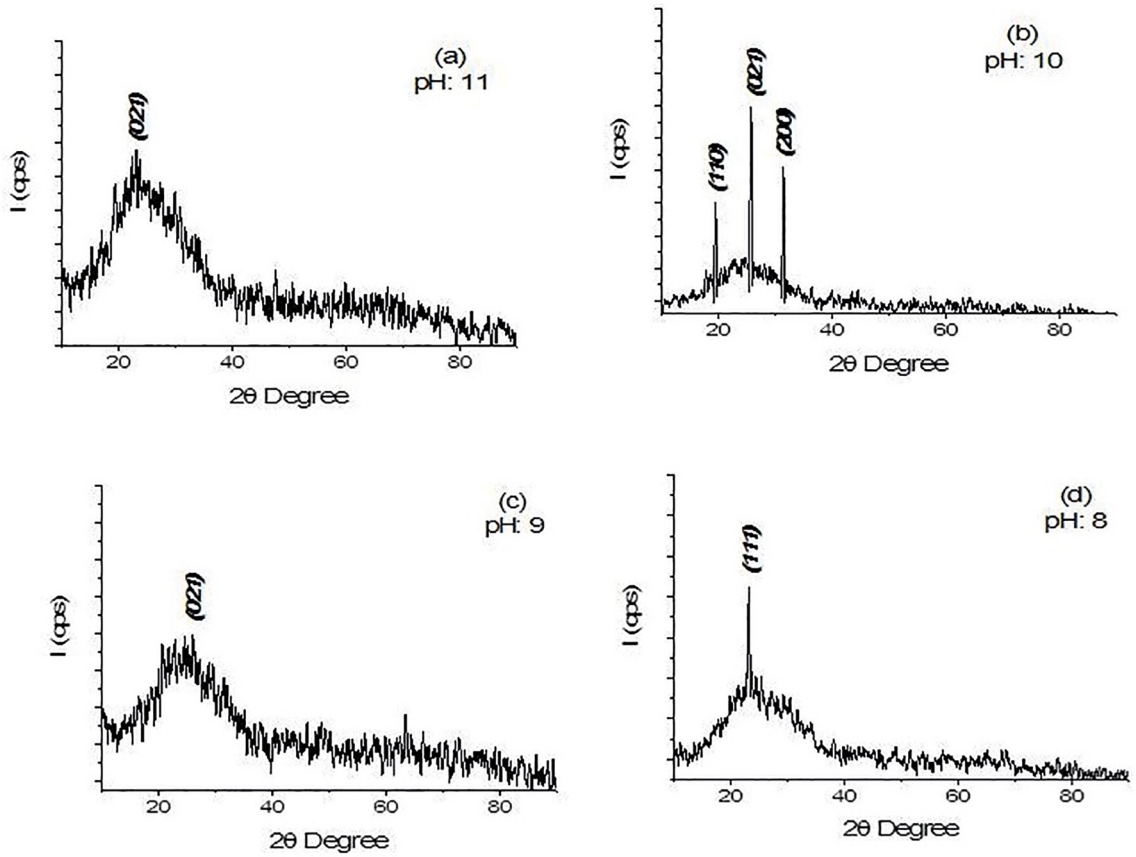

Figure 1. X-ray patterns of MnSeO4 films deposited at various pH levels: (a) pH 11, (b) pH 10, (c) pH 9 and (d) pH 8

Table 1. XRD datas of ASTM values versus films

pH	ASTM Data File	ASTM Value	Observed Value	Miller İndice
11	017-0840	25.42	26.43	$MnSeO_4$ (020)
10	017-0840	19.49	19.60	$MnSeO_4$ (110)
	017-0840	25.42	25.88	$MnSeO_4$ (021)
	017-0841	32.12	31.60	$MnSeO_4$ (110)
9	011-0683	28.29	27.72	$MnSeO_4$ (111)
8	011-0683	32.75	32.33	$MnSeO_4$ (022)

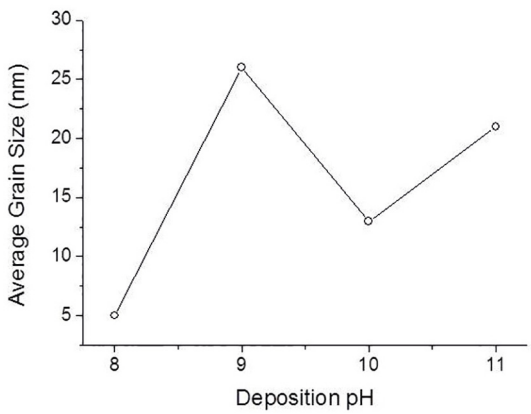

Figure 2. The grain size (D) of $MnSeO_4$ thin films deposited at various pH levels

of the wavelength[19]. The refraction indexes and extinction coefficients of the films are calculated by the formulas[16,17]:

$$n = \frac{(1+R)}{(1-R)} + \sqrt{\frac{4R}{(1-R)^2} - k^2} \qquad (6)$$

$$k = \frac{\alpha\lambda}{4\pi} \qquad (7)$$

The refraction index is shown in Figure 6. The refraction index and extinction coefficient of $MnSeO_4$ thin films were parallel with average grain size. The refraction indexes and extinction coefficients of $MnSeO_4$ films deposited at various pH levels were calculated as 1.53, 2.86, 2.07, 1.53

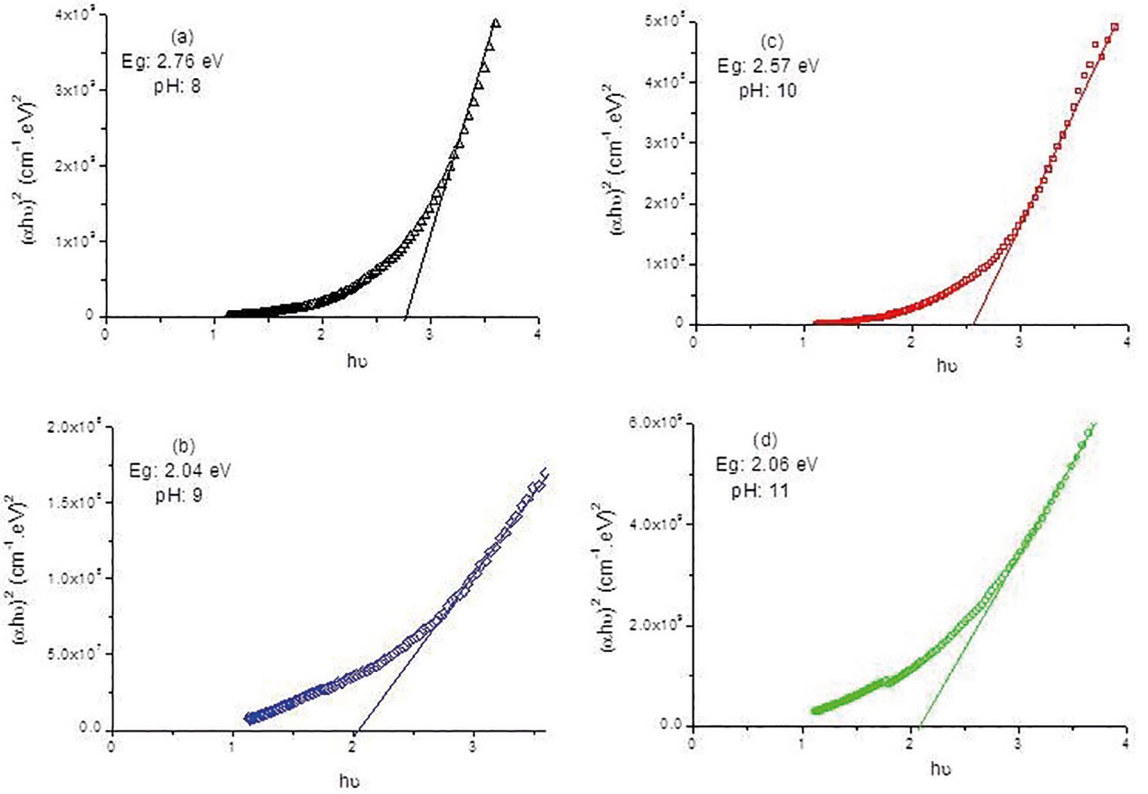

Figure 3. Plot of $(\alpha h\upsilon)^2$ vs. $h\upsilon$ for $MnSeO_4$ films deposited at various pH levels: (a) pH 11, (b) pH 10, (c) pH 9, (d) pH 8

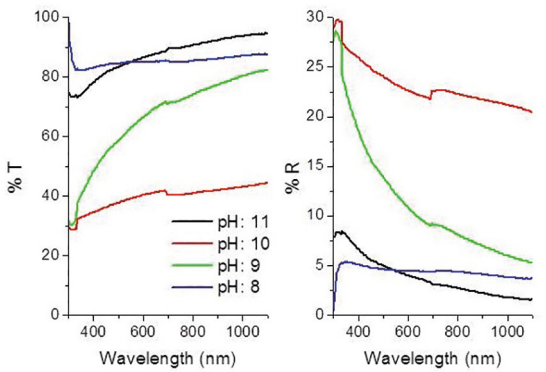

Figure 4. Transmittance and reflectance of $MnSeO_4$ thin films deposited at various pH levels

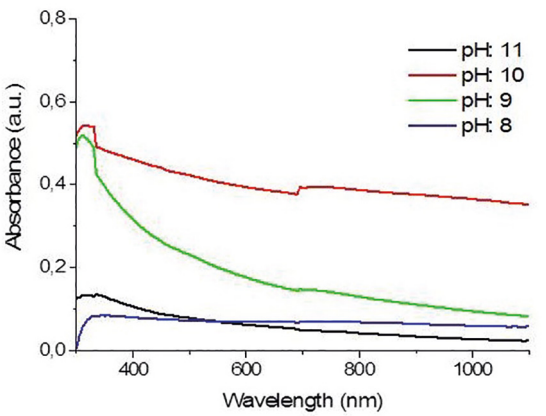

Figure 5. Absorbance of $MnSeO_4$ thin films deposited at various pH levels

(refraction index) – 0.005, 0.029, 0.014, 0.005 (extinction coefficient) at 550 nm wavelength, for average grain sizes of 21, 13, 26, and 5 nm. The values of refraction index and extinction coefficient show a natural behavior. Since the refraction of the light is bigger in scattered structure, the refraction index is higher for amorphous films.

The dielectric constant (ε) can be calculated using the following equation:

$$\varepsilon\varepsilon = \frac{4R}{1-R^2} - k^2 \qquad (8)$$

Dielectric constant also varied with the pH level of deposition bath and calculated to be 0.195, 1.575, 0.633 and 0.198 at 550 nm wavelengths (shown at Figure 7). Dielectric constant is a measure of vulnerability to the optical field. At 550 nm wavelengths, the highest dielectric constant was calculated for pH 10, where the highest peaks have also been observed. This fact was expected considering the orientation of the grains around the regular axis. The sum of the dipole moment vectors is higher at the film deposited at

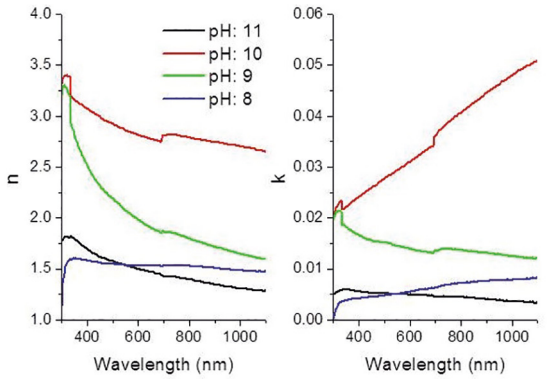

Figure 6. Plot of the refraction index and extinction coefficient of $MnSeO_4$ films deposited at various pH levels

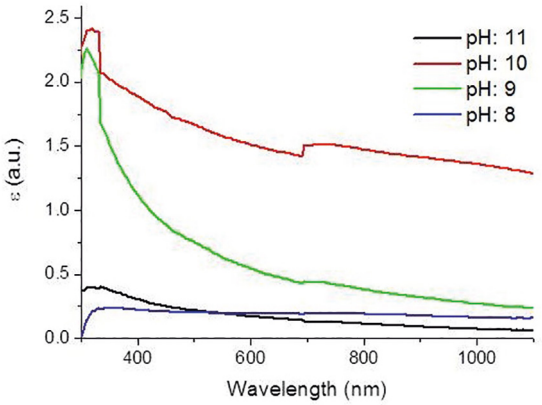

Figure 7. Plot of dielectric constant of MnSeO4 films deposited at various pH levels

pH 10 compared to the other films, so the interaction of the light with the particles was higher in this regular structure.

Table 2 shows EDX analysis of empty glass and $MnSeO_4$ thin film, which is a natural mineral, deposited on this glass. It will be a mistake to comment on the amount of oxygen due to the empty glass used for deposition. On the other hand, we cannot use the percentages of Mn and Se elements directly for other elements because of the contribution of the substrate, however we can calculate Se/Mn ratio theoretically from the chemical formulation of $MnSeO_4$. Theoretically Se/Mn ratio of this compound (in other words the ratio of the mass of the atomic weights in one mole) is 1.43. In our experimental analysis, this ratio was found to be 1.44, which is quite close to the theoretic ratio.

Natural $MnSeO_4$ mineral thin films may be very good alternatives for microelectronics world, where the materials with low dielectric constant are valuable (pH 8 and 11)[20]. A near-field optical technique, using a new type of solid immersion lens (using a SIL made from n=1.83 glass), applied to the writing and reading of domains in magneto-optic material (written and read 350 nm diameter magnetic

Table 2. EDX Analysis

	% Element	
Element	Empty Glass	$MnSeO_4$ Thin Film
Na	9,02	-
Mg	2,26	-
Al	0,72	-
Si	35,10	3,25
K	0,21	-
Cl	-	6,40
Ca	5,63	-
O	47,06	22,82
Se	-	32,53
Mn	-	32,59

domains), serves to increase the numerical aperture of the optical system by n, where n is the index of refraction of the lens material[21]. Because of the unavailability of optical materials with very low refraction indices that closely match the refraction index of air, such broadband antireflection coatings have not been realizable (pH: 8 and 11). Also, they demonstrate their potential for antireflection coatings by virtually eliminating Fresnel reflection from an AlN-air interface over a broad range of wavelengths[22]. The film of pH: 11 may be useful IR detectors because of higher transmission after the 700 nm wavelength (% T > 90)[23].

4. Conclusion

In this study, we tried to produce and investigate $MnSeO_4$ thin films, which were not studied by any researcher up to now. The films were produced at various pH levels, such as 11, 10, 9 and 8. Acidic values were not tried concerning about the formation of selenic acids in acidic environments. Optical properties of the films were investigated for various deposition pH's. Characteristics, such as optic band gap and refraction index were found to be in line with the average grain size and crystal structure of the films, moreover some of the results were compared with the literature. Most importantly, we do believe that a specific method has been discovered for the production of $MnSeO_4$ thin films. Considering their characteristics, these films are good candidates for the optical materials. In addition, it has been found that natural MnSeO4 mineral thin films have potential of being used as lens, magnetic-optic material and IR detector. The production methods of these kinds of different materials may be enlightening for the innovative researchers.

5. References

1. Natarajan S, Mandal S. Open-framework structures of transition-metal compounds. *Angewandte Chemie - International Edition*. 2008;47(26):4798-4828.

2. Rao CNR, Behera JN, Dan M. Organically-templated metal sulfates, selenites and selenates. *Chemical Society Reviews*. 2006;35(4):375-387.

3. Nabar MA, Paralkar SV. Thermal decomposition of some divalent metal selenates. *Thermochimica Acta*. 1975;11(2):187-196.

4. Pasha I, Choudhury A, Rao CNR. The first organically templated linear metal selenite. *Journal of Solid State Chemistry*. 2003;174(2):386-391.

5. Fujs S, Semenič T, Raspor P. The Effect of ATP Sulphurylase on the Prooxidant Properties of Selenate in Yeast Schizosaccharomyces pombe. *Food Technology and Biotechnology*. 2009;47(2):166-171.

6. Mittiga A, Salza E, Sarto F, Tucci M, Vasanthi R. Heterojunction solar cell with 2% efficiency based on a Cu_{2O} substrate. *Applied Physics Letters*. 2006; 88(16):163502.

7. Tanaka H, Shimakawa T, Miyata T, Sato H, Minami T. Effect of AZO film deposition conditions on the photovoltaic properties of AZO–Cu_2O heterojunctions. *Applied Surface Science*. 2005;244(1-4):568-572.

8. Katayama J, Ito K, Matsuoka M, Tamaki J. Performance of Cu_2O/ZnO Solar Cell Prepared By Two-Step Electrodeposition. *Journal of Applied Electrochemistry*. 2004;34(7):687-692.

9. Minami T, Tanaka H, Shimakawa T, Miyata T, Sato H. High-Efficiency Oxide Heterojunction Solar Cells Using Cu_2O Sheets. *Japanese Journal of Applied Physics*. 2004;43:L917-919.

10. Tanaka H, Shimakawa T, Miyata T, Sato H, Minami T. Electrical and optical properties of TCO–Cu_2O heterojunction devices. *Thin Solid Films*. 2004;469-470:80-85.

11. Siripala W, Ivanovskaya A, Jaramillo TF, Baeck SH, McFarland EW. A Cu_2O/TiO_2 heterojunction thin film cathode for photoelectrocatalysis. *Solar Energy Materials and Solar Cells*. 2003;77(3):229-237.

12. Papadimitriou L, Economou N, Trivich D. Heterojunction solar cells on cuprous oxide. *Solar Cells*. 1981;3(1):73-80.

13. Herion J, Niekisch EA, Scharl G. Investigation of metal oxide/cuprous oxide heterojunction solar cells. *Solar Energy Materials*. 1980;4(1):101-112.

14. Sears W, Fortin E, Webb J. Indium tin oxide/Cu_2O photovoltaic cells. *Thin Solid Films*. 1983;103(1-3):303-309.

15. Kariper IA. Pb-Ag/I Thin Film by Co-Precipitation Method. *Iranian Journal of Science and Technology, Transactions A: Science*. 2016;40:137-143.

16. Kariper IA. Optical and structural properties of chromium telluride (Cr_2Te_3) thin film produced via chemical bath deposition. *Optoelectronics and Advanced Materials-Rapid Communications*. 2016;10(7-8):541-546.

17. Kariper IA. Production and characterization of Tel_x (x: 2, 4) thin films: Optical, structural properties and effect of porosity. *Materials & Design*. 2016;106:170-176.

18. Kariper IA. CuI Film Produced by Chemical Extraction Method in Different Media. *Materials Research*. 2016;19(5):991-998.

19. Ramana CV, Smith RJ, Hussain OM. Grain size effects on the optical characteristics of pulsed-laser deposited vanadium oxide thin films. *Physica Status Solid A*. 2003;199(1):R4-R6.

20. Maex K. Low dielectric constant materials for microelectronics. *Journal of Applied Physics*. 2003;93(11):8793-1841.

21. Terris BD, Mamin HJ, Rugar D, Studenmund WR, Kino GS. Near-field optical data storage using a solid immersion lens. *Applied Physics Letters*. 1994;65(4):388-390.

22. Xi JQ, Schubert MF, Kim JK, Schubert EF, Chen M, Lin SY, et al. Optical thin-film materials with extremely low refractive index for broadband elimination of Fresnel reflection. *Nature Photonics*. 2007;1:176-179.

23. Plyler EK, Blaine LR. Transmittance of Materials in the Far Infrared. *Journal of Research of the National Bureau of Standards-C*. 1960;64C(1):55-56.